Removal of Textile Dye from Aqueous Solution Using Immobilized Cells on Column pozzolana Bed Reactor

[1,2] Cherifi Souad*, [2]Djafer Abderrahmane, [1]Mehdaoui Razika, [3]Sameut Bouhaik Izzeddine, [4]Fizir Meriem and [5]Iddou Abdelkader

[1] Laboratory of Natural Products Chemistry and Biomolecules, Faculty of Sciences University of Blida 1, BP 270 Blida Algeria

[2]Laboratoire Eau et Environnement, Hassiba Ben Bouali University of Chlef.

[3]Laborotory for theorical physics and material physics, Hassiba Ben Bouali University of Chlef.

[4]Laboratoire de Valorisation des Substances Naturelles, Khemis Miliana University, 44225 Khemis Miliana,, Algeria.

[5]Laboratoire Ressources Naturelles Sahariennes, Faculté des Sciences et de la Technologie, Université Ahmed Draia – Adrar 01000, Algeria.

s.cherifi@univ-dbkm.dz*

Summary: Textile dyes are hazardous and carcinogenic materials. Hence, their removal from wastewater is globally required. This research aims to remove anionic dye red bemacid E-TL from aqueous solutions using a biofilm supported on granular pozzolana in a fixed-bed column. The effect of different experimental conditions such as influent dye concentrations, flow rate and bed depth on red bemacid biosorption at room temperature were investigated. Results indicated that the breakthrough and saturation time increase with the decrease of the flow rate. The same effect is shown when the bed depth is increased. Favorable conditions for dye removal were observed with 60 cm of column height, lowest flow rate 1mL/min and initial red bemacid concentration of 60 mg/L; at which the highest removal efficiency of 52,68% were recorded. The breakthrough data obtained for RB E-TL removal fitted Thomas and Yoon-Nelson model with high correlation coefficients ($R^2 = 0,992$). The results obtained proved that fixed microorganisms biomass could be a promising biosorbent for the removal of red bemacid from aqueous solutions in a dynamic process.

Keywords: Biosorption; Biomass; Breakthrough curves; Packed column; Biofilm

Introduction

Nowadays, contamination of the environment and human health is serious crisis facing our universe due to the pollution of aquatic ecosystems by industrial effluents containing high levels of synthetic dyes [1]. This kind of effluent would impart a significant color to water even at a very low dose, causes not only aesthetic damage, but also prevents the sun-light transmission through water [2], which leads to a suppression of photosynthetic activities of aquatic plants [3] and increasing the biological oxygen demand. Furthermore, the textile dyes have hazardous outcomes, particularly mutagenic and carcinogenic [4]. These pollutants could damage the DNA once they have being ingested by human body and metabolized by intestinal microorganisms. Therefore, proper treatment of textile wastewater is crucial to remove residual dyes before the effluents are discharged into the environment [5].

Various techniques including ion exchange [6], adsorption [7, 8], electrochemical [9-12], electrochemical advanced oxidation [13], chemical oxidation [14], precipitation [15], membrane filtration [16], coagulation [17], electrolysis [18], fenton and photo fenton process

[19] were adopted to remove dyes from industrial effluents. Unfortunately, these techniques are limited due to their costs, excessive consumption of chemicals, and complexities in treatment procedure especially when applied to high-throughput contaminated water. Currently, using biosourced or natural mineral materials such as algae, wool waste, agricultural waste (i.e corn ear, hulls of nuts-and rice husk), waste activated sludge, and waste biomass from commercial bioprocesses, etc., as adsorbents has attracted considerable interest for the removal of contaminants from industrial sewage, particularly for heavy metals and dyes [20-24] because of its many advantages including high efficiency, selectivity and energy savings. Biosorption of dye, i.e., the used of microorganisms for decolorizing textile wastewater is considered relatively cost-effective and nature-friendly. This approach can eliminate dyes completely from wastewaters. In addition, the toxic intermediate and dyes byproducts could be mineralized by the microbial biomass as well. Several microbial have been tested including yeasts, algae, fungi, bacteria and actinomycetes for efficient dye removal [25-28]. Under optimal conditions, the adaptability and the activity of studied

microorganism is the key feature of the microbial decolorization efficiency. However, free cells exploited for industrial scale purpose have some operational drawbacks such as cell toxicity, shear force, cell stability in stirring conditions and biomass-effluent separation. An immobilized bacterial cell was suggested to overcome the aformontioned issues and its application for dyes remediation paves widespread research attention recently due to its outstanding stability, regeneration, reuse and easier solid-liquid separation [29]. Packed bed column with continuous flow process are more efficient in large-scale industrial wastewater management, as it makes best use of the concentration difference which is the driving force for pollutants uptake and thus of the capacity of adsorbent can be utilized efficiently [30, 31]. Furthermore, large volume of effluents can be continuously managed using a predetermined amount of sorbent in a packed bed column [32]. However, limited reports employed packed bed columns for dyes removal [32-34]. In this context, calcium alginate immobilized microorganism in packed bed column showed high removal efficiency of various contaminants such as cupper and chrome [35]. In another research, entire decolorization and COD removal of Methyl orange (300 mg/L) was achieved in a packed bed reactor using alginate immobilized Aeromonas sp [29]. Recently, flay ash was also used as support material for pseudomonas attachment to treat congo red dye [36] . It is evident from the above literature that synthetic materials were widely used as support for microbial immobilization which needs a higher energy and chemical products consumption. Thus, researchers have long been committed to apply a natural and low cost supports for bioremediation of dyes from water. Pozzolana is a natural porous and homogeneous rock of volcanic origin which is ecofriendly, abundant in nature and relatively inexpensive. Despite of this inert material showed a high removal capacity of various pollutants from wastewaters [37, 38], limited studies investigate it as support for continuous biological elimination of dyes from water. Our research group removed about 90% of Cr (VI) from water using the immobilized yeast onto pozzolana [39]. Based on these encouraging results, this work aims is to study the ability of microbial biomass bed column for remove an industrial organic dye, Red Bemacid E-TL in aqueous solution through dynamic method. The effects of several parameters, such as RB E-TL concentration, flow rate, and column bed depth were investigated using the same column and the same support at laboratory scale fixed-bed column. The experimentally obtained results were analyzed using models of Adams-Bohart, Thomas, Yan and Yoon–Nelson.

Experiment

Materials

Preparation of RB E-TL dye solution

The pollutant model RB E-TL dye (Commercial name Red Bemacid E-TL) $C_{24}H_{20}O_6N_4S_2NaCl$, is an industrial synthetic dye which was obtained from the textile manufacturing situated in the Tlemcen city (West Algeria). It was purchased from Bezema society, with a molar weight of 583 g/mol and purity of 99%. Red Bemacid is soluble in water and was used directly in the experiment without pre-treatment. An aqueous stock solution was prepared by dissolving 500 mg/L in double distilled water. Different experiments were conducted using diluted solutions from the aformontioned stock solution which is conserved at 4°C.

Preparation of biomass

A microbial biomass used in this study was obtained from domestic wastewater treatment plant. The microbial strain was grown aerobically at room temperature in culture broth consisting of a base mix of casein- peptone 0.2 g/L; glucose 1 g/L; NH_4NO_3 0.0571 g/L and to the final KH_2PO_4 0.035 g/L (one liter of tap water was used to dissolve the mixture) [40].

Fixed-bed column studies

The support was Granular pozzolana with an average size of 3 mm and 4 m^2/g area. The particle size of the support was measured using the sieving process. The chemical composition of pozzolana was determined using the XRD Philips PW 3710 X-ray apparatus and textural characteristics calculated from nitrogen adsorption isotherms is carried out with an ASAP 2010 Micrometric device. The results are summarized in Table-1.

Pozzolana was watched with distilled water, in order to eliminate any pollutant in the pores, and then sterilised at 110°C for 120 min. After that, 60 g of the support were placed in a‒cylindrical plastic column having inside diameter 2.5 cm and length 80 cm (Fig. 1). In order to distribute the solution uniformly over the entire cross section of the column, a plastic sieve plate was filed at the bottom of the column and glass beads of 0.5-0.6 cm diameter were placed above the sieve plate. Nutrient broth and microorganisms were pumped (upward flow) at a rate of 8 mL/min for 3 days, aiming the optimisation of the adhesion and the growth of the biofilm (Fig. 2). The high flow rate (8 mL/min) is used to allow the formation of a compact biofilm and resistant to the erosion stress. Binocular magnifier was used to screen the biofilm formation on the pozzolana.

Table-1: Composition (wt%) and textural characteristics of pozzolana.

Adsorbent	Chemical composition (Wt%)									Textural properties		
	Al_2O_3	SiO_2	Fe_2O_3	Na_2O	CaO	MgO	K_2O	SO_3	WL	S_{BET} (m^2/g)	V_{Pores} (cm^3/g)	D_{Pores} (A°)
Pozzolana	17,50	46,10	10,50	3,40	10,50	3,80	1,50	0,40	4,41	4	0,011	109,58

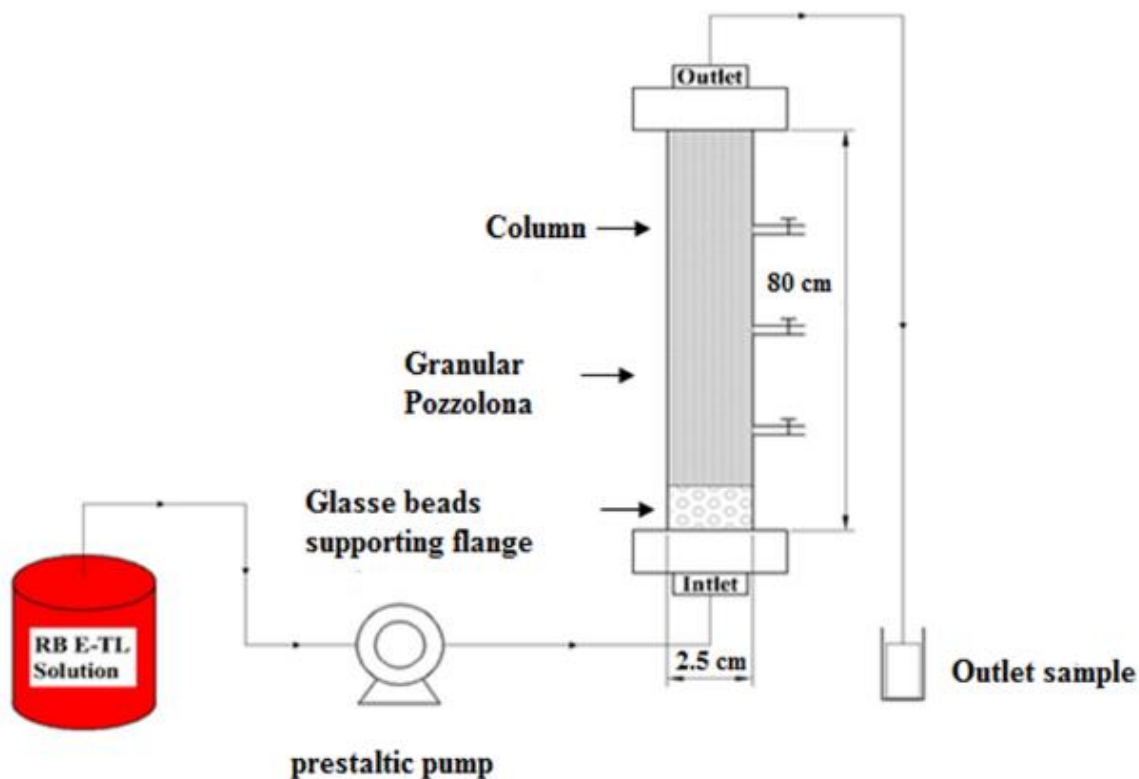Note: WL: weight loss at 900˚C.

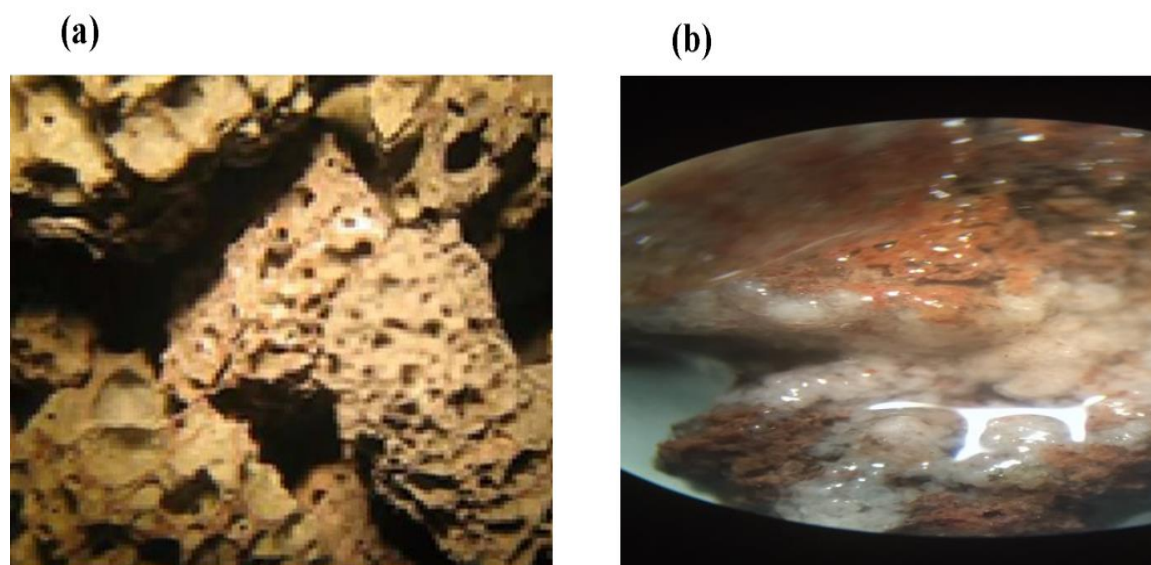Fig. 1:   Schematic diagram for the fixed bed column.

Fig. 2:   Pozzolana aspect (a) before and (b) after the biofilm formation.

After biofilm formation, the aqueous solution of RB E-TL dye was pumped to bed using a peristaltic pump (Prominent, model E2100). Different experimental parameters were evaluated to assess the biofilm performance, bed heights (H= 20, 40 and 60 cm), flow rate (1- 4 L/min) and initial RB E-TL concentration (40-100 mg/L). pH of the solution in this experiment was ranging from 6.5 to 7.

At the end of each assay, column was washed with nutrient broth at the high flow (8ml/min) to reduce biofilm thickness, slow down his maturation and maintain the biofilm by reducing bacterial diversity [41]. It is worth mentioning that the biofilm is not regenerated. It is washed frequently to reduce its thickness. The residue entrained in the washing water is dried and then destroyed. This is referred to large sewage treatment plants that use the trickling filter process. The concentration of intel and residual dye in the supernatant was measured by OPTIZEN 2010 spectrophotometer at 504 nm [40].

Column data analysis

Breakthrough curves have been used to predict fixed bed efficiency and are constructed by plotting the C_t/C_0 ratio as a function of time or effluent volume. Column parameters were determined as described below [42] .

The volume of the effluent, V_{eff} (mL), can be measured from the following equation:

$$V_{eff} = Q.t_{total} \tag{1}$$

where Q is the volumetric flow rate (mL/min) and t_{total} is the total flow time (min).

The total amount of red bemacid dye (m_{total}) added to the column (mg) is expressed by equation (2).

$$m_{totale} = \frac{C_0 Q t_{total}}{1000} \tag{2}$$

The total weight of RB E-TL removal by immobilized cells in the column, i.e. q_{total} (mg), for a given feed concentration and flow rate, is equal to the area under the plot of the adsorbed RB E-TL concentration, C_{ad} (C_o-C_t) (mg/L) versus t (min), is calculated by equation (3)

$$q_{total}(mg) = \frac{Q}{1000} \int_{t=0}^{t=t_{total}} C_{ad} \, dt \tag{3}$$

The total RB E-TL removal (% removal) is calculated by equation (4)

$$R_c(\%) = \frac{q_{total}}{m_{totale}} \times 100 \tag{4}$$

Fixed-Bed Modeling

The dynamic performance of the column can be predicted using various empirical mathematical models including the Yoon-Nelson, the Thomas, the Yan and Bohart-Adams models. The linear equation of each model is depicted in Table-2; where C_t and C_0 are the outlet and the inlet concentration respectively in the solution (mg/L), t is the sampling time (min), k_{YN} (L/min) is the Yoon-Nelson constant, τ (min) is the time in required for 50% adsorbate breakthrough, k_{Th} is Thomas rate constant (ml/mn.g), q_0 is the maximum capacity of adsorption (mg/g), m is the mass of adsorbent packed in the column (g), Q is feed flow rate (ml/min), K_{AB} is the kinetic constant (L/mg.min), N_0 is the saturation concentration (mg/L), Z is the bed depth in the column (m), U is the linear flow rate (m/mn), a is an experimental parameter that set the slope of the regression function.

Table-2: List of continuous adsorption models.

Model	Linear equation	Reference
Yoon–Nelson	$\ln\frac{C_t}{C_0 - C_t} = K_{YN} t - \tau K_{YN}$	[43]
Thomas	$\ln(\frac{C_\circ}{C_t} - 1) = \frac{k_{Th} q_0 m}{Q} - k_{Th} C_0 t$	[44]
Bohart –Adams	$\ln\frac{C_t}{C_0} = K C_0 t - K N_0 \frac{Z}{U}$	[45]
Yan	$Ln\left(\frac{C_t}{C_0 - C_t} - 1\right) = a \, Ln\left(\frac{0,001 Q C_0}{q_0 m}\right) + a \, Ln \, t$	[46]

Results and Discussion

Effect of initial dye concentration. Influent dye concentration is among the important parameters affecting operating characteristics in column fixed-bed biosorption, because it offers a significant driving force to overcome all mass transfer resistance of dye between the aqueous solution and the bulk phases [47]. The impact of initial RB E-TL dye concentration (40, 60, 80, and 100 mg/L) on breakthrough curves at a constant bed height of 20 cm and influent flow rate of 1 mL/min is depicted in Fig. 3a. The parameters of the column are illustrated in Table-3. Fig.3a showed that the fixed bacterial bed was exhausted faster at the higher inlet concentration RB E-TL dye. Curves demonstrated that the breakthrough point was reached promptly with 100 mg/L solution than with the other concentrations. It is clear that the breakthrough time decreased from 150 to 10 min with increasing dye concentration at the inlet due to the rapid saturation of the binding sites on the cells wall in the column at high dyes concentration. This resulted in a shorter bed breakthrough and exhaustion time [48]. Furthermore, it was noted that a decrease in adsorbate concentration provided an extended breakthrough curve, illustrating that a higher volume of solution could be treated. This fact can be explained by a decrease in diffusion coefficient lead to slower transport which is resulted from the lower concentration gradient [49, 50]. The total RB E-TL (q_{total}) adsorbed found to be decreased from 10,631 to 9,412 mg causing a decrease in the efficiency of dyes removal from 66, 44 to 27, 68 %, when the concentration augmented from 40 to 100 mg/L.

Effect of flow rate. The flow rate was varied from 1 to 4 mL/min to investigate the effect of flow rate on the removal of RB E-TL dye, whereas initial feed concentration and the bed height were held constant at 60 mg/L and 20 cm, respectively. The breakthrough curve is illustrated in Fig. 3b and Table-3. The breakthrough time decreased from 65 to 12 min as the flow rate increased from 1 to 4 mL/min and the removal efficiency decreased from 49, 69 to 26, 30 % with increasing flow rate. The decrease in the dye uptake capacity at higher flow rates can be explained as follow: (i) Interaction of solute with the sorbent is limited due the unavailability of sufficient retention time and (ii) the incomplete diffusivity of solute into the binding sites of the biomass caused thereby.

On the other hand, higher adsorption capacity of (49,69 %) at lower flow rate (1mL/min) can be explained by the availability of additional residential time for cells to remove RB E-TL from solution [51].

Effect of bed depth. The amount of the biosorbent inside the packed bed column is the key feature for an efficient dyes biosorption and reduction. The study was conducted for three different bed heights 20, 40 and 60 cm using 60, 120 and 180 g of pozzolana respectively as a support for biomass. A flow rate of 1 mL/min of dye solution with an initial concentration of 60 mg/L was fixed as the feed conditions for the column studies. As shown in Fig. 3c and Table-3, the removal efficiency increase with increasing bed height. This behavior is due to the microorganisms reflecting the increasing of the number of binding sites in the biofilm. However, the higher bed depths supplies longer breakthrough times as the dyes molecules needed sufficient residence time to diffuse profoundly into the inner surface of fixed biomass. The removal efficiency of dye obtained respectively was 49,69, 50,13 and 52,68% for bed heights of 20, 40 and 60 cm.

Table-3: The parameters of the fixed-bed column for the RB E-TL dye removal at different conditions, inlet concentrations C_0 (mg/L), flow rates Q (mL/min), and bed heights H (cm).

C_0 (mg/L)	Q (mL/min)	H (cm)	t_{total} (min)	V_{eff} (mL)	m_{total} (mg)	q_{total} (mg)	R (%)
40	1	20	400	400	16	10,631	66,44
60	1	20	400	400	24	11,926	49,69
80	1	20	400	400	32	12,277	38,36
100	1	20	340	340	34	9,412	27,68
60	1	20	400	400	24	11,926	49,69
60	2	20	400	800	48	16,238	33,82
60	4	20	400	1600	96	25,253	26,30
60	1	20	400	400	24	11,926	49,69
60	1	40	480	480	28,8	14,440	50,13
60	1	60	560	560	33,6	17,701	52,68

Modeling of breakthrough curves

This part presents the digital models allowing access to the pollutant concentration profile at the outlet of the adsorption column.

Bohart – Adams, Thomas and Yoon -Nelson models that are considered as simple mathematical models have been developed to determine the column dynamic behavior and to calculate approximately some kinetic coefficients.

We used in this study, four mathematical models recently developed from the equations developed by the models Adams and Bohart (1920), Thomas (1944), Yoon-Nelson and Yan to describe and estimate the experimental data concluded from dynamic investigations realized on a fixed bed to predict breakthrough curves. The values of the parameters of Thomas (K_{TH}, q_0), Adams and Bohart (K_{AB}, N_0), Yoon and Nelson (K_{YN}, τ) and Yan (a, q_0), the correlation coefficients of the regression (R^2) are presented in Tables 4 and 5 respectively. The breakthrough curve at different initial red bemacid concentration, feed flow rate and column bed height is shown in Fig. 4, 5, 6 and 7.
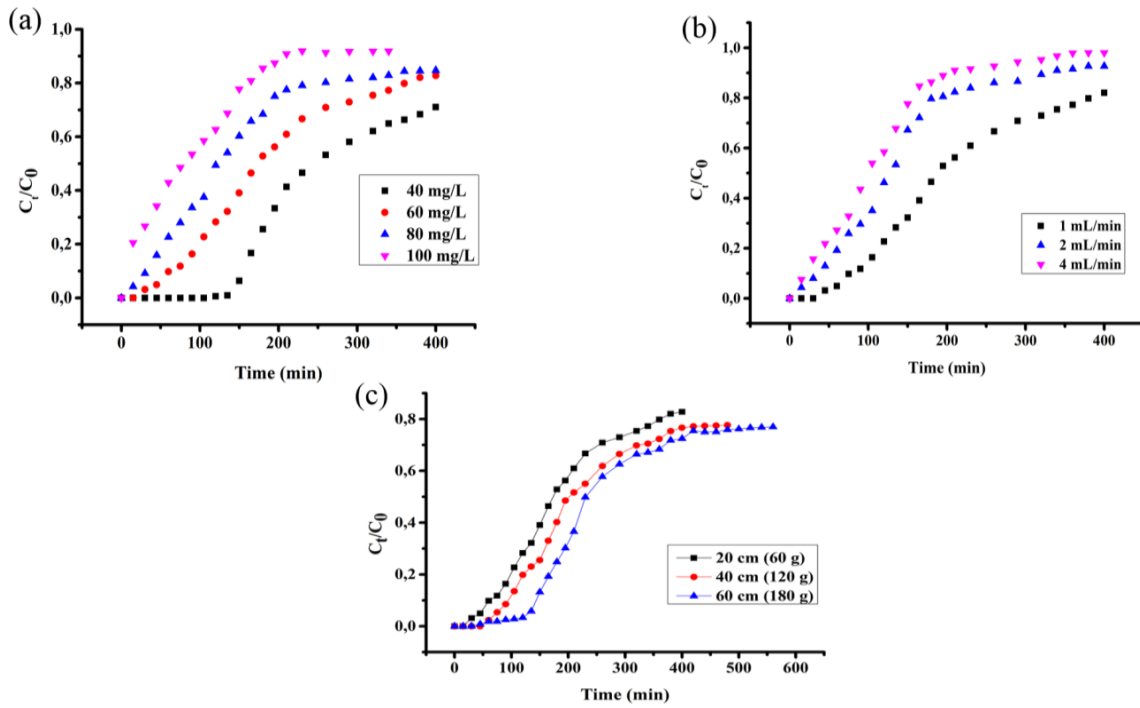
Fig. 3:   Breakthrough curves for the removal of RB E-TL dye by immobilized cells in columns at (a) different inlet concentrations (Q = 1 mL/min, H = 20 cm); (b) different flow rate (C_0 = 60 mg/L, H = 20 cm); (c) different heights (C_0 = 60 mg/L, Q = 1 mL/min).
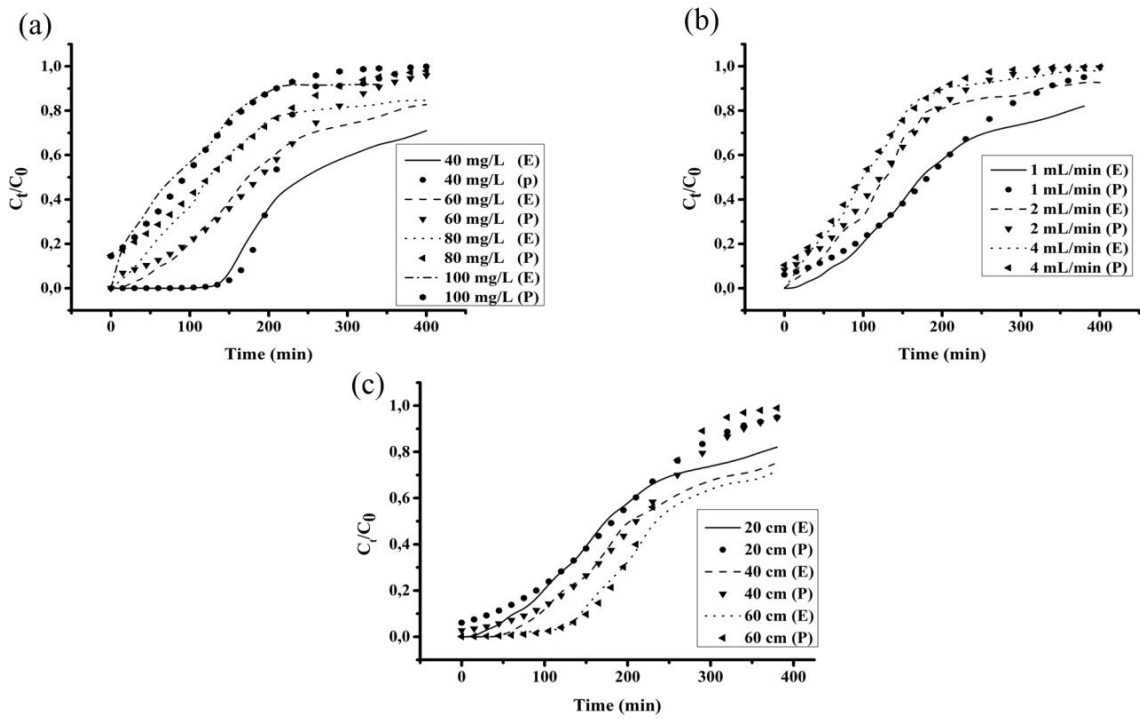

Fig. 4:   Thomas model fitting of the experimental data for red bemacid on a biofilm supported on granular pozzolana using different (a) initial feed concentration, (b) feed flow rate and (c) column bed height.
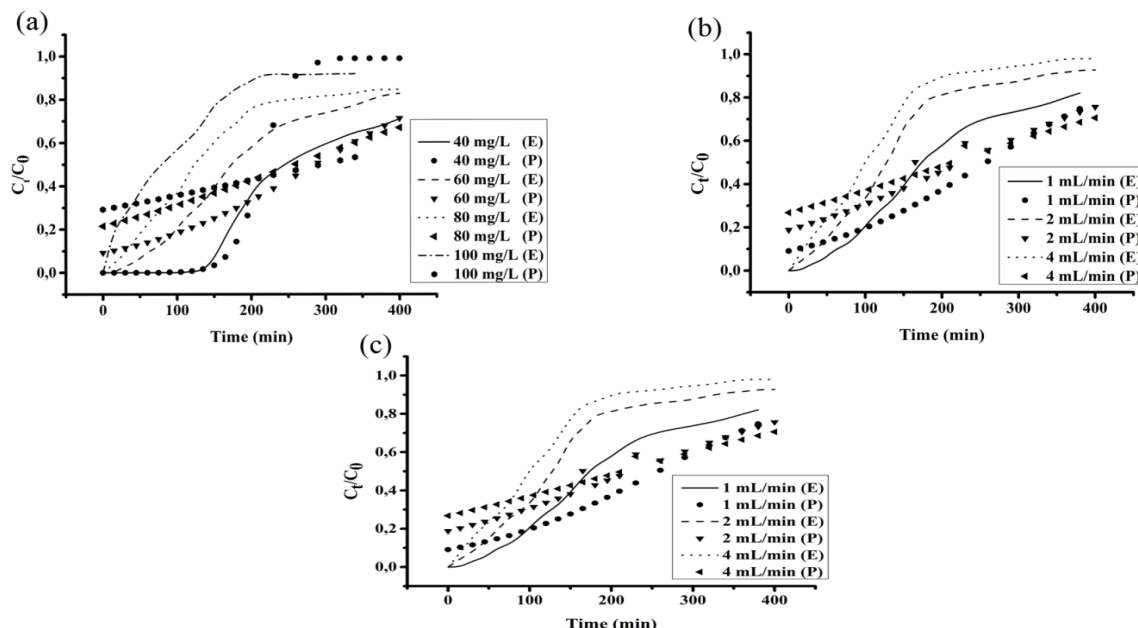
Fig. 5:   Adams–Bohart model fitting of the experimental data for red bemacid on a biofilm supported on granular pozzolana using different (a) initial feed concentration, (b) feed flow rate and (c) column bed height

Thomas Model. From the results presented in Table-4, K_{Th} and q_o values of the Thomas model decreased with increasing of the initial red bemacid concentration. These findings are similar to those reported by Salah Bensadek et al.[52], it was attributed to the driving force for adsorption in the concentration difference. As the flow rate increased, the value of K_{TH} increased whiles the value of q_0 increased. Thomas' constants increase and the maximum adsorbed amounts decrease with increasing bed height, the same result was obtained by Chen et al. [53]. The values of the correlation coefficients $R^2 = 0, 99$, Thomas' model also describes all of the red bemacid breakthrough curves well (Fig 4). It is clear that this model is well applied in the adsorption of continuous RB-ETL. These results show that Thomas' model is representative of our system. As shown in Table-6, the adsorption capacity of the immobilized cells on the pozzolana is higher than other used biosorbent in dynamic process.

Adams–Bohart Model. The R^2 values of Adams–Bohart model were in the range of 0,86–0,984. The average regression value was 0,932. According to regression value, Adams–

Bohart model is not fitting to the data point well (Fig 5). Table-4 also shows an increase in adsorption capacity with increasing flow rate and initial concentration. Similar results were obtained by Ahmad and Hameed, (2010) in the case of the

adsorption of dyes on activated carbon [49]. Moreover, an opposite effect is observed with the height of the bed, a decrease in the adsorption capacity with increase in the kinetic constant as found by previous reports [30, 54, 55]. Chen et al. stated that the external mass transfer is localized in the initial part of the column which resulted in a dominant global kinetics of the system. This phenomena is due to the increased of K_{AB} with increasing bed depth which is similar with our results [56].

Yoon-Nelson model. The results of Table-5 indicated that the value of (τ) considerably decreased as the influent dye concentration increased, because the rapid column saturation [57]. On the other hand, with the increase in the flow rate lead to a decrease in the constant of proportionality (K_{YN}) and a decrease in time (τ). As for the increase in the height of the bed, we note an increase in K_{YN} and τ. The increase in τ indicates that saturation occurs more slowly with increasing bed height. While the force that controls the phenomenon of mass transfer in the liquid phase could explain the increase in k_{YN}[58]. These results are similar with those found by previous works [54, 59-61]. The high values of the regression coefficient indicate that the Yoon-Nelson model adequately describes the experimental results for the three parameters examined (Fig. 6).

Yan Model. There is a decrease in adsorption capacity and a decrease in the empirical parameter "a"

of Yan with increasing dye concentration, the same result was obtained with increasing bed height. As shown in Fig. 7, the experimental data fitted no very well with the Yan model for all the experimental conditions studied. The R^2 values were in the range of 0,5–0,97. Therefore, the experimental data obtained from biosorption of RB E-TL fitted no very well with Yan biosorption model. It is obvious from the regression coefficients that Thomas and Yoon Nelson's models are the most representative compared to other, and the most adopted to describe the phenomenon of RB E-TL retention on a biofilm

supported on granular pozzolana. The adsorption process can be explained and the longevity of the bed in the field scale could be estimated by using the aformontioned models.

Table-4. Correlation parameters of Thomas and Adams–Bohart models for adsorption of red bemacid E-TL on a biofilm supported on granular pozzolana at varying influent red bemacid concentration, feed flow rate and column bed height.
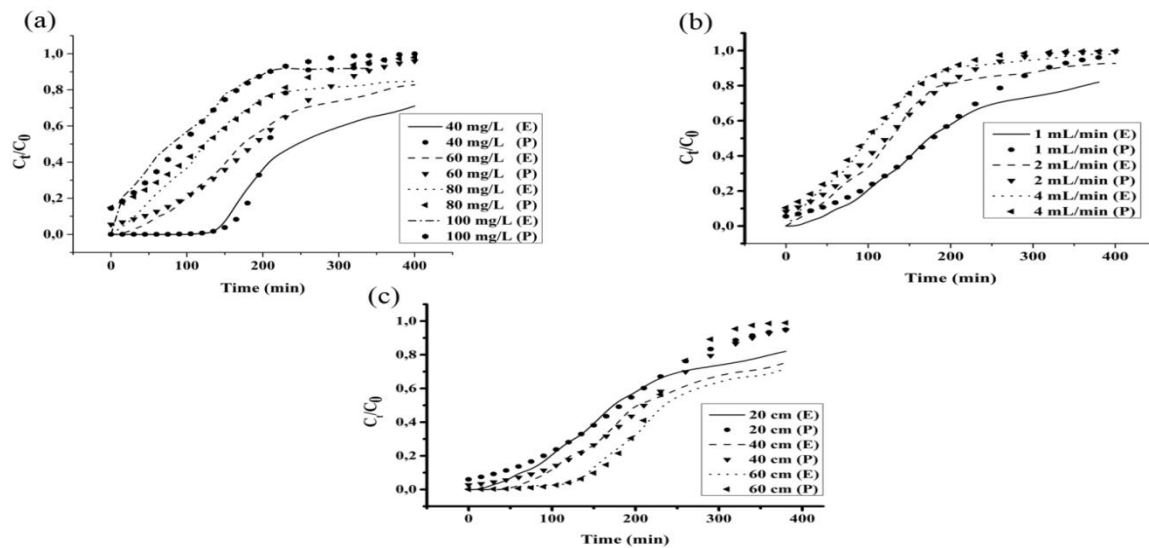

Fig. 6: Yoon-Nelson model fitting of the experimental data for red bemacid on a biofilm supported on granular pozzolana using different (a) initial feed concentration, (b) feed flow rate and (c) column bed height.
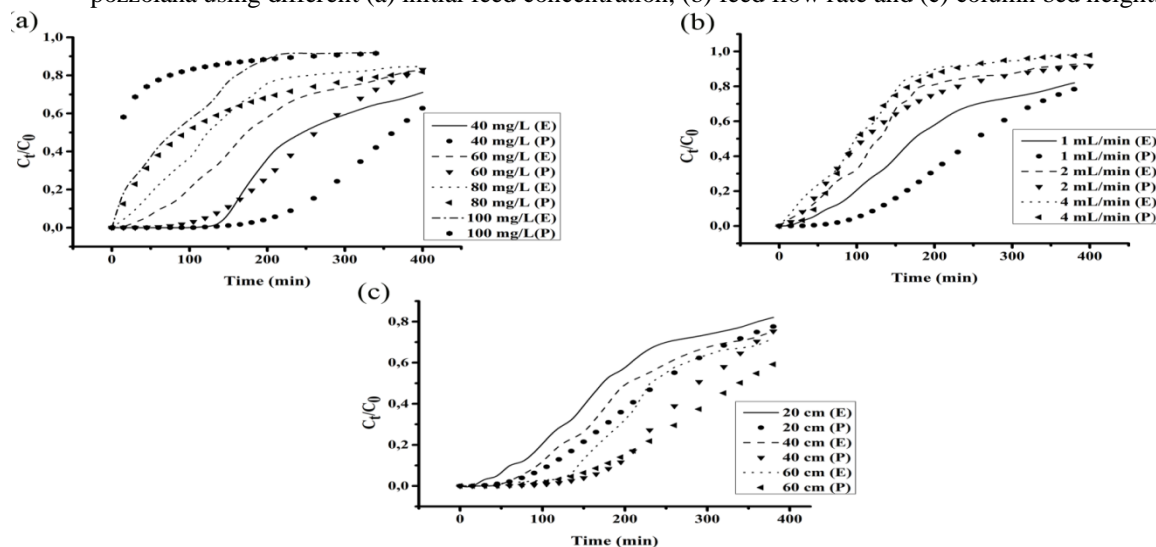

Fig. 7: Yan model fitting of the experimental data for red bemacid on a biofilm supported on granular pozzolana using different (a) initial feed concentration, (b) feed flow rate and (c) column bed height.

Table-4: Correlation parameters of Thomas and Adams–Bohart models for adsorption of red bemacid E-TL on a biofilm supported on granular pozzolana at varying influent red bemacid concentration, feed flow rate and column bed height.

C_0 (mg.L^{-1})	H (cm)	Q (ml.min^{-1})	Thomas Model			Adams–Bohart model		
			$K_{TH}.10^{-4}$ (mL.mn^{-1}.g^{-1})	q_0 (mg.g^{-1})	R^2	$K_{AB}.10^{-4}$ (l.mg^{-1}.mn^{-1})	N_0 (mg.L^{-1})	R^2
40	20	1	14,25	138,362	0,928	12,75	156,591	0,899
60	20	1	2,5	182,133	0,99	1,48	280,978	0,97
80	20	1	1,75	166,285	0,992	0,625	375,648	0,978
100	20	1	1,9	155,614	0,989	0,3	536,9	0,888
60	20	1	2,5	182,133	0,99	1,48	280,978	0,97
60	20	2	3,3	243,131	0,941	1,08	491,914	0,88
60	20	4	3,65	392,675	0,97	0,78	930,889	0,86
60	20	1	2,5	182,133	0,99	1,48	280,978	0,97
60	40	1	2,83	105,094	0,982	1,91	143,038	0,984
60	60	1	5,16	74,084	0,949	4,33	88,308	0,925

Table-5: Correlation parameters of Youn Nelson and Yan models for adsorption of red bemacid E-TL on a biofilm supported on granular pozzolana at varying influent red bemacid concentration, feed flow rate and column bed height.

C_0 (mg.L^{-1})	H (cm)	Q (ml.min^{-1})	Youn Nelson Model			Yan model		
			K_{YN} (L.mn^{-1})	τ (mn)	R^2	a	q_0	R^2
40	20	1	0,056	207,857	0,918	5,145	0,242	0,946
60	20	1	0,015	177,636	0,99	3,18	0,252	0,93
80	20	1	0,014	124,785	0,992	1,05	0,126	0,97
100	20	1	0,019	93,263	0,989	0,66	0,015	0,5
60	20	1	0,015	177,636	0,99	3,18	0,252	0,93
60	20	2	0,012	121,560	0,94	1,87	0,219	0,98
60	20	4	0,013	98,173	0,97	2,79	0,405	0,94
60	20	1	0,015	177,636	0,99	3,18	0,252	0,93
60	40	1	0,017	204,188	0,983	4,87	0,159	0,90
60	60	1	0,031	219,530	0,95	3,28	0,113	0,94

Table-6: Comparison of maximum sorption capacity of immobilized cells on granular pozzolana in a fixed bed column with other biosorbents

Dye	Bisorbent	q_0 (mg/g) according to Thomas	Reference
Brilliant Red HE-3B	*Bacillus* sp. Consortia biomass immobilized in an alginate	38.05	[62]
malachite green	*Bacillus cereus* M$^1_{16}$ immobilized in calcium alginate	37.21	[35]
Reactive Red 198 (RR198)	microbial cell-immobilized *Platanus orientalis* leaf tissue (NSPOL)	50.92	[63]
Reactive Yellow 2 (RY2)	microbial cell-immobilized *Platanus orientalis* leaf tissue (NSPOL)	46.45	[63]
Red Bemacid E-TL	microorganisms immobilized on the pozzolana	74.21	This work

Mechanisms for the degradation of red bemacid E-TL

In the literature, the complete degradation or "mineralization" of azo dyes by microorganisms (bacteria) is described by the succession of two essential steps: anaerobic azoreduction followed by aerobic oxidation of the aromatic amines formed during the previous step. Azoreduction is described as the key step in the mineralization of dyes, in particular this step is sufficient for the discoloration of molecules [64]. In the anaerobic condition, the dye reduction was carried out by specific azoreductase enzyme. By contrast, in the aerobic condition, there is no specific enzyme to cleave the azo-bond (–N=N–). The anaerobic dye reduction can be done in three different ways as shown in figure 8. The azoreduction reaction can occur both intracellularly and extracellularly, the electron donors (ED) can be NADH, NADPH or FADH, and as these cofactors are located in the cytoplasm, the reaction need a redox mediator (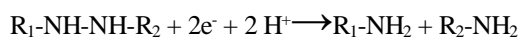RM) to carry the electrons from the oxidoreductase enzymes located in cytoplasmic membrane to the dye in extracellular environment. The redox mediator must have a redox potential between –430 and –180 mV. The direct dye reduction is possible by specific transport system that permit the uptake of the RB-ETL dye into the cells or by lysis of cells that release the cofactors at extracellular environment [64-67].

The azoreduction phenomenon requires a transfer of four electrons in two stages. In each stage, two electrons are given to the azo dye which is in fact a final electron acceptor [66, 69].

Step 1: Hydrazo intermediate

$$R_1\text{-N=N-}R_2 + 2e^- + 2\,H^+ \longrightarrow R_1\text{-NH-NH-}R_2$$

Step 2: Reductive cleavage of the azo bond

$$R_1\text{-NH-NH-}R_2 + 2e^- + 2\,H^+ \longrightarrow R_1\text{-NH}_2 + R_2\text{-NH}_2$$
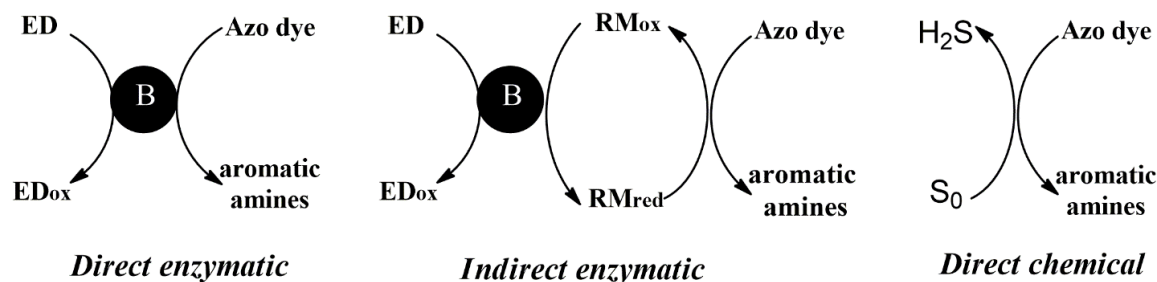
Fig. 8:   Schematic illustration of the different mechanisms of anaerobic azo dye reduction,
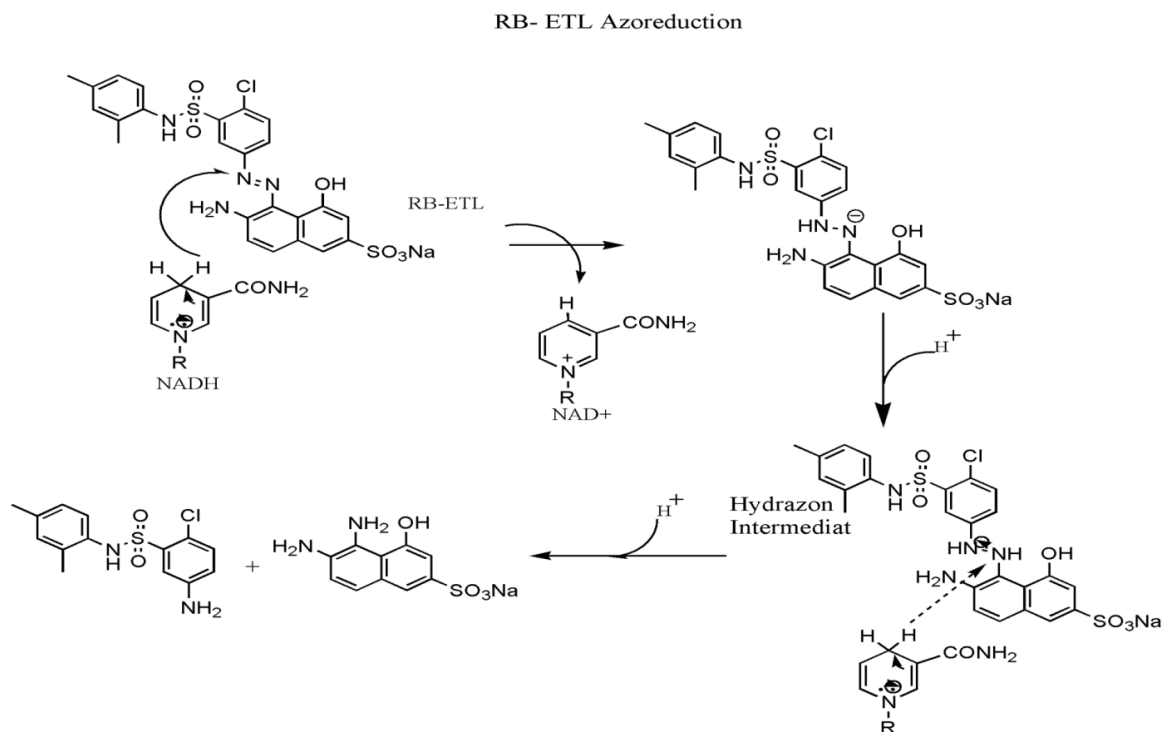B = bacteria; ED = electron donor; RM = redox mediator [68].

Fig. 9:   Direct azo reduction of RB-ETL by NADH.

The mechanism of direct RB-ETL reduction by NADH as suggest is shown in Fig 9.

In the case of sulfonated azo dye like RB E-TL, another intermediate step is proposed before the cleavage of azo bond. Based on computational chemistry calculation, Mendoza-Huizar (2014) suggests the protonation of sulfonate groupmind before the cleavage of azo bond [70].

As perspective of this work, we will use computational chemistry calculation to propose a detailed mechanism of RB E-TL degradation by using fixed microorganisms (biofilm), and understand the relation dye structure–biodegradability. The understanding of relation structure-reactivity of RB E-TL

help to develop more performance process of wastewater treatment or propose new dye to the industry that will be no toxic and more biodegradable

Conclusion

The current research demonstrated the efficiency of microorganisms immobilized on the pozzolana for the elimination of an industrial dye in aqueous solution in column. The results revealed that the maximum biosorption capacity of 74.21 mg/g was attained at optimum conditions (dye concentration of 60 mg/L, lowest flow rate of 1 mL/min and bed height of 60 cm). Process modeling makes it possible to successfully design a column for industrial operation. The experimental data are adequate to Yoon-Nelson and

Thomas models for all conditions with regression coefficients of 0.99. The efficiency of the biofilm is 52.68%. Thus, cells immobilized on pozzolana can be considered as a promising biosorbent for the removal of red bemacid dye that could be used in industrial and environmental remediation.

References

1. A.Tkaczyk, K. Mitrowska and A. Posyniak, Synthetic organic dyes as contaminants of the aquatic environment and their implications for ecosystems: a review, *Sci. Total Environ.*, **717**, 137222 (2020).

2. M.M. Hassan and C.M. Carr, A critical review on recent advancements of the removal of reactive dyes from dyehouse effluent by ion-exchange adsorbents, *Chemosphere.*, **209**, 201 (2018).

3. A. Djafer, L. Djafer, B. Maimoun, A. Iddou, S. Kouadri Mostefai and A. Ayral, Reuse of waste activated sludge for textile dyeing wastewater treatment by biosorption: performance optimization and comparison, *Water Environ J.*, **31**, 105 (2017).

4. K. Piaskowski, R. Świderska-Dąbrowska and P.K. Zarzycki, Dye removal from water and wastewater using various physical, chemical, and biological processes, *J. AOAC Int.*, **101**, 1371 (2018).

5. T. Adane, A.T. Adugna and E. Alemayehu, Textile industry effluent treatment techniques, *J. Chem.*, **2021**, (2021).

6. Y. Jia, L. Ding, P. Ren, M. Zhong, J. Ma and X. Fan, Performances and mechanism of methyl orange and Congo red adsorbed on the magnetic ion-exchange resin. *J. Chem. Eng*. Data., **65**, 725 (2020).

7. R. A. Akbour, H. Ouachtak, A. Jada, S.Akhouairi, A. A. Addi, J. Douch and M. Hamdani, Humic acid covered alumina as adsorbent for the removal of organic dye from coloured effluents, *Desalin. Water Treat.*, **112**, 207 (2018).

8. J. El Gaayda, , R. A. Akbour, F. E. Titchou, H. Afanga, H. Zazou, C. Swanson and M. Hamdani, Uptake of an anionic dye from aqueous solution by aluminum oxide particles: equilibrium, kinetic, and thermodynamic studies, *Mediterr. J. Chem. Groundw. Sustain. Dev.*, **12**, 100540 (2021).

9. S. Palanisamy, P. Nachimuthu, M. K. Awasthi, B. Ravindran, S. W. Chang, M. Palanichamy and D. D. Nguyen, Application of electrochemical treatment for the removal of triazine dye using aluminium electrodes, *J. Water Supply: Res. Technol. – AQUA.*, **69**, 345 (2020).

10. S. El-Kacemi, H. Zazou, N. Oturan, M. Dietze, M. Hamdani, M. Es-Souni and M. A. Oturan, Nanostructured ZnO-TiO$_2$ thin film oxide as anode material in electrooxidation of organic pollutants. Application to the removal of dye Amido black 10B

11. F. E. Titchou, H. Afanga, H. Zazou, R. A. Akbour and M. Hamdani, Batch elimination of cationic dye from aqueous solution by electrocoagulation process, *Mediterr. J. Chem.* **10**, 1-12 (2020).

12. F. E. Titchou, H. Zazou, H. Afanga, , J. El Gaayda, R. A. Akbour, M. Hamdani and M. A. Oturan, Electro-Fenton process for the removal of Direct Red 23 using BDD anode in chloride and sulfate media, *J. Electroanal. Chem.*, **897**, 115560 (2021).

13. F. E. Titchou, H. Zazou, H. Afanga, J. El Gaayda, R. A. Akbour, P. V. Nidheesh and M. Hamdani, An overview on the elimination of organic contaminants from aqueous systems using electrochemical advanced oxidation processes, *J. Water Process. Eng.*, **41**, 102040 (2021).

14. J. Li, K. Zhu, R. Li, X. Fan, H. Lin and H. Zhang, The removal of azo dye from aqueous solution by oxidation with peroxydisulfate in the presence of granular activated carbon: Performance, mechanism and reusability, *Chemosphere.*, **259**, 127400 (2020).

15. A. Reyes-Serrano, J. E. López-Alejo, M. A. Hernández-Cortázar and I. Elizalde, Removing contaminants from tannery wastewater by chemical precipitation using CaO and Ca (OH)$_2$, *Chin. J. Chem. Eng.*, **28**, 1107 (2020).

16. L. Semiz, Removal of reactive black 5 from wastewater by membrane filtration, *Polym. Bull.*, **77**, 3047 (2020).

17. F. Mcyotto, Q. Wei, D. K. Macharia, M. Huang, C. Shen and C. W. Chow, Effect of dye structure on color removal efficiency by coagulation, *Chem. Eng. J.*, **405**, 126674 (2021).

18. L. Liu, D. He, F. Pan, R. Huang, H. Lin and X. Zhang, Comparative study on treatment of methylene blue dye wastewater by different internal electrolysis systems and COD removal kinetics, thermodynamics and mechanism, *Chemosphere.*, **238**, 124671 (**2020**).

19. A. Sennaoui, S. Alahiane, F. Sakr, A. Assabbane, E. H. A. Addi and M. Hamdani, Advanced oxidation of reactive yellow 17 dye: a comparison between Fenton, photo-Fenton, electro-Fenton, anodic oxidation and heterogeneous photocatalysis processes, *Port. Electrochimica Acta.*, **36**, 163 (2018).

20. D. de Vasconcelos, G. Maria, J. Mulinari, A. A. Ulson de Souza, D. de Oliveira and C. J. de Andrade, Biodegradation of azo dye-containing wastewater by activated sludge: a critical review, *World J. Microbiol. Biotechnol.*, **37**, 1-12 (2021).

21. B. Brazesh, S. M. Mousavi, M.Zarei, M. Ghaedi, S. Bahrani and S. A. Hashemi, Biosorption, *Interface Sci. Technol.*, 33, 587 (2021).

22. B. Van Veenhuyzen, S. Tichapondwa, C. Hörstmann, E. Chirwa and H. Brink, High capacity Pb (II) adsorption characteristics onto raw-and chemically activated waste activated sludge, *J. Hazard. Mater.*, **416**, 125943 (2021).

23. N. Asim, M.H. Amin, M. Alghoul, S.N.A. Sulaiman, H. Razali, M. Akhtaruzzaman, N. Amin, K. Sopian, Developing of chemically treated waste biomass adsorbent for dye removal, *J. Nat. Fibers.*, **18**, 968 (2021).

24. P. K. Yeow, S. W. Wong and T. Hadibarata, Removal of azo and anthraquinone dye by plant biomass as adsorbent—a review, *Biointerface Res. Appl. Chem.*, **11**, 8218 (2021).

25. Y. Patel, U. Chhaya, D. M. Rudakiya and S. Joshi, In *Microbial Rejuvenation of Polluted Environment*, *Biological Decolorization and degradation of synthetic dyes: a green step toward sustainable environment*, Springer, p. 77 (2021).

26. Y. Tak, M. Kaur, J. Tilgam, H. Kaur, R. Kumar and C. Gautam, In *Bioremediation of Environmental Pollutants*, *Microbes Assisted Bioremediation: A Green Technology to Remediate Pollutants*, Springer, p 25 (2022).

27. M. Danouche, H. El Arroussi, W. Bahafid and N. El Ghachtouli, An overview of the biosorption mechanism for the bioremediation of synthetic dyes using yeast cells, *Environ. Technol. Rev.*, **10**, 58 (2021).

28. S. Devanshi, K. R. Shah, S. Arora and S.Saxena, In *Crude Oil-New Technologies and Recent Approaches Actinomycetes as An Environmental Scrubber*, IntechOpen (2021).

29. M. N. Kathiravan, S. A. Praveen, G. H.Gim, G. H. Han and S. W. Kim, Biodegradation of Methyl Orange by alginate-immobilized Aeromonas sp. in a packed bed reactor: external mass transfer modeling, *Bioprocess Biosyst. Eng.*, **37**, 2149 (2014).

30. S. Adhikari, P. Chattopadhyay and L. Ray, Continuous removal of malathion by immobilised biomass of Bacillus species S14 using a packed bed column reactor, *Chem. Speciat. Bioavailab.*, **24**, 167 (2012).

31. S. Adhikari, P. Chattopadhyay and L. Ray, Biosorption of Malathion using dry cells of Bacillus species S14 in a packed bed column reactor, *Chem. Speciat. Bioavailab.*, **25**, 273 (2013).

32. Z. Aksu, G. Eğretli and T. Kutsal, A comparative study of copper (II) biosorption on Ca-alginate, agarose and immobilized C. vulgaris in a packed-bed column, *Process Biochem.*, **33**, 393 (1998).

33. A. Saeed, M. Iqbal and S. I. Zafar, Immobilization of Trichoderma viride for enhanced methylene blue biosorption: Batch and column studies, *J. Hazard. Mater.*, **168**, 406 (2009).

34. K. Vijayaraghavan and Y.-S Yun, Polysulfone-immobilized Corynebacterium glutamicum: a biosorbent for Reactive black 5 from aqueous solution in an up-flow packed column, *Chem. Eng. J.*, **145**, 44 (2008).

35. J. Nath, L. Ray and D. Bera, Continuous removal of malachite green by calcium alginate immobilized Bacillus cereus M_{16}^1 in packed bed column, *Environ. Technol. Innov.*, **6**, 132 (2016).

36. S. Desireddy and S. Pothanamkandathil Chacko, *In Dye Biodegradation, Mechanisms and Techniques, Hybrid Bioreactors for Dye Biodegradation*, Springer, p 263 (2022).

37. G. Derouich, S. A. Younssi, J. Bennazha, B. Achiou, M. Ouammou, I.-E. E. A. El Hassani and A. Albizane, Adsorption study of cationic and anionic dyes onto Moroccan natural pozzolan. Application for removal of textile dyes from aqueous solutions, *Desalination Water Treat*, **145**, 348 (2019).

38. F.E. Titchou, R.A. Akbour, A. Assabbane and M. Hamdani, Removal of cationic dye from aqueous solution using Moroccan pozzolana as adsorbent: isotherms, kinetic studies, and application on real textile wastewater treatment, *Groundw. Sustain. Dev.*, **11**, 100405 (2020).

39. A. Djafer, S. K. Moustefai, A. Idou and M. Douani, Batch and continuous packed column studies biosorption by yeast supported onto granular pozzolana. *WASET*, **7**, 665 (2013).

40. A. Djafer, S. Kouadri Moustefai, A. Iddou, and B. Si Ali, Study of bimacid dye removal from aqueous solution: a comparative study between adsorption on pozzolana, bentonite, and biosorption on immobilized anaerobic sulfate-reducer cells, *Desalination Water Treat.*, **52**, 7723 (2014).

41. A. Rochex, J.-J. Godon, N. Bernet and R. Escudié, Role of shear stress on composition, diversity and dynamics of biofilm bacterial communities, *Water Res.*, **42**, 4915 (2008).

42. F.E. Titchou, H. Zazou, H. Afanga, J. El Gaayda, R.A. Akbour and M. Hamdani, Removal of persistent organic pollutants (POPs) from water and wastewater by adsorption and electrocoagulation process, *Groundw. Sustain. Dev.*, **13**, 100575 (2021).

43. Y.H. Yoon and J.H. NELSON, Application of gas adsorption kinetics—II. A theoretical model for respirator cartridge service life and its practical applications, *Am. Ind. Hyg. Assoc. J.*, **45**, 517 (1984).

44. H.C. Thomas, Heterogeneous ion exchange in a flowing system, *J. Am. Chem. Soc.*, **66**, 1664 (1944).

45. G. Bohart and E. Adams, Behavior of charcoal towards chlorine, *J. Am. Chem. Soc.* **42**, 523 (1920).

46. G. Yan, T. Viraraghavan and M. Chen, A new model for heavy metal removal in a biosorption column, *Adsorpt. Sci. Technol.*, **19**, 25 (2001).

47. S. Baral, N. Das, T. Ramulu, S. Sahoo, S. Das and G.R. Chaudhury, Removal of Cr (VI) by thermally activated weed Salvinia cucullata in a fixed-bed column, *J. Hazard. Mater.*, **161**, 1427 (2009).

48. S. Hasan, D. Ranjan and M. Talat, Agro-industrial waste 'wheat bran'for the biosorptive remediation of selenium through continuous up-flow fixed-bed column, *J. Hazard. Mater.*, **181**, 134 (2010).

49. A. Ahmad and B. Hameed, Fixed-bed adsorption of reactive azo dye onto granular activated carbon prepared from waste, *J. hazard. Mater.*, **175**, 298 (2010).

50. Z. Chowdhury, S. Zain, A. Rashid, R. Rafique and K. Khalid, Breakthrough curve analysis for column dynamics sorption of Mn (II) ions from wastewater by using Mangostana garcinia peel-based granular-activated carbon, *J. Chem.*, **2013**, (2013).

51. P. Suksabye, P. Thiravetyan and W. Nakbanpote, Column study of chromium (VI) adsorption from electroplating industry by coconut coir pith, *J. Hazard. Mater.*, **160**, 56 (2008).

52. S. Bensadek, H. Aguedal, A. Iddou and A. Aziz, Biosorption of Chromium (VI) in a Fixed-Bed Column Using Adsorbent Biomass, *Key Eng. Mater.*, **800**, 157 (2019).

53. S. Chen, Q. Yue, B. Gao, Q. Li, X. Xu and K. Fu, Adsorption of hexavalent chromium from aqueous solution by modified corn stalk: a fixed-bed column study, *Bioresour. Technol.*, **113**, 114 (2012).

54. K. Sankar, S.K. Rajaram, I.G. Moorthy, K. Naresh, S. Vaitheeswaran, R.A. Kumar, G.M. Viyas and P.K.J. Samuel, In *Sustainable Development in Energy and Environment, Continuous Sorption of Chlorpyrifos from Aqueous Solution Using Endoskeleton Powder of Sepia officinalis,* Springer, p 225, (2020).

55. J. López-Cervantes, D.I. Sánchez-Machado, R.G. Sánchez-Duarte and M.A. Correa-Murrieta, Study of a fixed-bed column in the adsorption of an azo dye from an aqueous medium using a chitosan–glutaraldehyde biosorbent, *Adsorpt. Sci. Technol.*, **36**, 215 (2018).

56. C.-Y. Chen, H.-W. Chang, P.-C. Kao, J.-L. Pan and J.-S. Chang, Biosorption of cadmium by CO_2-fixing microalga Scenedesmus obliquus CNW-N, *Bioresour. Technol.*, **105**, 74 (2012).

57. M. Calero, F. Hernáinz, G. Blázquez, G. Tenorio and M. Martín-Lara, Study of Cr (III) biosorption in a fixed-bed column, *J. Hazard. Mater.*, **171**, 886 (2009).

58. C.A. Demarchi, A. Debrassi, J. Dal Magro, N. Nedelko, A. Ślawska-Waniewska, P. Dłużewski, J.-M. Greneche and C.A. Rodrigues, Adsorption of Cr (VI) on crosslinked chitosan–Fe (III) complex in fixed-bed systems, *J. Water Process. Eng.*, **7**, 141 (2015).

59. Z. Aksu and F. Gönen, Biosorption of phenol by immobilized activated sludge in a continuous packed bed: prediction of breakthrough curves, *Process Biochem.*, **39**, 599 (2004).

60. W. Zhang, L. Dong, H. Yan, H. Li, Z. Jiang, X. Kan, H. Yang, A. Li and R. Cheng, Removal of methylene blue from aqueous solutions by straw based adsorbent in a fixed-bed column, *Chem. Eng. J.*, **173**, 429 (2011).

61. A. Aichour, H. Zaghouane-Boudiaf, F.B.M. Zuki, M.K. Aroua and C.V. Ibbora, Low-cost, biodegradable and highly effective adsorbents for batch and column fixed bed adsorption processes of methylene blue, *J. Environ. Chem. Eng.*, **7**, 103409 (2019).

62. L.I. Horciu, C. Zaharia, A.C. Blaga, L. Rusu and D. Suteu, Brilliant Red HE-3B Dye Biosorption by Immobilized Residual Consortium Bacillus sp. Biomass: Fixed-Bed Column Studies, *Appl. Sci.*, **11**, 4498 (2021).

63. S. Celik, N. Duman, F. Sayin, S.T. Akar and T. Akar, Microbial cells immobilized on natural biomatrix as a new potential ecofriendly biosorbent for the biotreatment of reactive dye contamination, *J. Water Process. Eng.*, **39**, 101731 (2021)

64. F.P. Van der Zee, G. Lettinga and J.A. Field, Azo dye decolourisation by anaerobic granular sludge, *Chemosphere.*, **44**, 1169 (2001).

65. R. Russ, J. Rau and A. Stolz, The function of cytoplasmic flavin reductases in the reduction of azo dyes by bacteria, *Appl. Environ. Microbiol.*, **66**, 1429 (2000).

66. A.B. Dos Santos, F.J. Cervantes and J.B. Van Lier, Review paper on current technologies for decolourisation of textile wastewaters: perspectives for anaerobic biotechnology, *Bioresour. Technol.*, **98**, 2369 (2007).

67. S. Singh, S. Chatterji, P. Nandini, A. Prasad and K. Rao, Biodegradation of azo dye Direct Orange 16 by Micrococcus luteus strain SSN2, *Int. J. Environ. Sci. Technol.*, **12**, 2161 (2015).

68. A. Pandey, P. Singh and L. Iyengar, Bacterial decolorization and degradation of azo dyes, *Int. Biodeterior. Biodegradation.*, **59**, 73 (2007).

69. P.K. Singh and R.L. Singh, Bio-removal of azo dyes: a review, *Int. j. appl. sci. biotechnol.*, **5**, 108 (2017).

70. L.H. Mendoza-Huizar, A theoretical study of chemical reactivity of tartrazine through DFT reactivity descriptors, *J Mex Chem Soc.*, **58**, 416 (2014).